LIMNOLOGY
AND
OCEANOGRAPHY

January 2006
Volume 51
Number 1

Limnol. Oceanogr., 51(1), 2006, 1–11

Testing the effect of CO_2 concentration on the dynamics of marine heterotrophic bacterioplankton

Hans-Peter Grossart[1]
Leibniz Institute of Freshwater Ecology and Inland Fisheries, Department of Limnology of Stratified Lakes, Alte Fischerhuette 2, 16775 Stechlin, Germany

Martin Allgaier
Leibniz Institute of Freshwater Ecology and Inland Fisheries, Department of Limnology of Stratified Lakes, Alte Fischerhuette 2, 16775 Stechlin, Germany

Uta Passow
Alfred Wegener Institute for Marine and Polar Research, Am Handelshafen 12, 27570 Bremerhaven, Germany

Ulf Riebesell
Leibniz Institute for Marine Sciences, University of Kiel, Duesternbrooker Weg 20, 24105 Kiel, Germany

Abstract

To date no study exists that directly addresses changes in dynamics of heterotrophic bacteria in surface waters in relation to partial pressure of CO_2 (pCO_2). Therefore, we studied the effect of changes in pCO_2 on bacterial abundance and activities by using mesocosms with different pCO_2 levels (~190, ~370, and ~700 ppmV, representing past, present-day, and future atmospheric pCO_2, respectively). Abundance of total bacteria did not differ with increasing pCO_2 throughout the whole study period, whereas bacterial protein production (BPP) was highest at highest pCO_2. This effect was even more pronounced for cell-specific production rates, especially those of attached bacteria, which were up to 25 times higher than those of free bacteria. During the breakdown of the bloom, however, the abundance of both free and attached bacteria was significantly increased with pCO_2. Differences in bacterial growth rate (μ) were smaller than those of BPP, but both μ and BPP of attached bacteria were elevated under high pCO_2. Averages of total protease as well as α- and β-glucosidase activities were highest at elevated pCO_2 levels, but a statistically significant dependence on pCO_2 was only evident for protease activity. There is a measurable but indirect effect of changes in pCO_2 on bacterial activities that are mainly linked to phytoplankton and presumably particle dynamics.

The world's oceans are currently absorbing one third of the anthropogenic carbon emissions each year and will presumably absorb even higher percentages in the near future. According to the Intergovernmental Panel on Climate Change (IPCC scenario IS92a, Houghton et al. 2001), surface water CO_2 concentrations will increase by almost threefold at the end of this century as compared with preindustrial values. This will result in a pH drop by ca. 0.35 units by the year 2100 (Wolf-Gladrow et al. 1999). According to another study (Caldeira and Wickett 2003), pH values may

[1] Corresponding author (hgrossart@igb-berlin.de).

Acknowledgments

We thank the staff of the Large Scale Facility (LFS) in Bergen, in particular Jorun Egge and Celia Booman for their great help in conducting our study. Kirsten Pohlmann is thanked for statistical analyses and comments on an earlier version of the manuscript, and Scarlett Trimborn for Chl *a* measurements and field assistance. We are grateful to all other participants of the PeECE (Pelagic Ecosystem CO_2 Enrichment) study for their valuable technical assistance, data acquisition, and discussions. We appreciate the helpful comments of two anonymous reviewers.

This work was supported by the Alfred Wegner Institute for Polar and Marine Research. Access to installations from the University of Bergen and from the Institute of Marine Research has been funded by the Improving Human Potential Programme from the European Union through contract HPRI-CT-2002-00181.

even drop by 0.7 units over the next two centuries, which may have no analog over the past 300 million years. The majority of CO_2 absorbed by the ocean will initially be stored in the upper 200 m, with the potential to influence pelagic ecosystems in surface waters.

There are many recent studies on phytoplankton carbon acquisition mechanisms that indicate large effects on physiology and composition due to changes in aquatic pCO_2 (e.g., Burkhardt et al. 2001; Tortell et al. 2002). A doubling in present CO_2 levels will result in a significant reduction of biogenic calcification of Foraminifera and coccolithophores (Bijma et al. 1999; Riebesell et al. 2000). Reduced calcification by planktonic organisms and a suggested higher loss of POC at high pCO_2 (Engel et al. 2005) significantly lowers the vertical transport of calcium carbonate (and hence alkalinity) to the deep sea and overall particle flux to deeper waters (Armstrong et al. 2002; Klaas and Archer 2002). On the other hand, differences in CO_2 uptake rates seem to influence the production of extracellular organic matter (e.g., an increase in concentration of transparent exopolymer particles [TEP] with increasing pCO_2 (Engel 2002; Engel et al. 2004). Several studies indicate that TEP are major components of marine aggregates and that they are enriched in carbon relative to nitrogen or phosphorus (Engel and Passow 2001; Mari et al. 2001). Thus, the C : N : P ratio of sinking particles in the ocean may also be sensitive to changes in surface water CO_2 concentration. These changes in quantity and quality of dissolved and particulate organic matter may substantially impact activities of free and particle-associated bacteria.

In terrestrial ecosystems such as soil and peat bog systems, increasing levels in pCO_2 often lead to increased bacterial numbers and activities that can be either linked to increasing photosynthetic exudation (Zak et al. 2000) or to changes in peroxidase activities. Although heterotrophic bacteria play a major role in organic matter cycling in marine pelagic ecosystems (e.g., Cole et al. 1988; Azam 1998), there are only speculations on the effect of increased oceanic pCO_2 on dynamics of heterotrophic bacteria. Until now, only one study has shown a direct effect of decreased seawater pH from CO_2 dissolution on bacterial production in the deep sea (Coffin et al. 2004). An increase in bacterial production was observed at all temperatures at a slightly elevated pH if cells were repressurized. In another study (Rochelle-Newall et al. 2004), abundances of total bacteria and concentrations of chromophoric dissolved organic matter (CDOM) in mesocosms were independent of pCO_2. To reliably predict bacterioplankton dynamics in the presence of increased oceanic pCO_2, there is a great need for repeated studies under controlled environmental conditions. Therefore, we have used mesocosms with CO_2 concentrations adjusted to glacial (190 ppmV), present (370 ppmV), and future (700 ppmV) pCO_2 levels (Houghton et al. 2001). By using a nutrient ratio with elevated levels of silicate, we intended to initiate the development of a diatom bloom and to monitor the temporal course of several ecosystem parameters, in particular bacterial abundance, production, and hydrolytic ectoenzyme activities. Our study shows that changes in pCO_2 levels lead to significant differences in bacterial activities, especially of attached bacteria.

Materials and methods

Experimental set up—This study was part of the outdoor mesocosm project Pelagic Ecosystem CO_2 Enrichment Study (PeECE) conducted in the Raunefjorden (60.3°N, 5.2°E) at the Large Scale Facility in Bergen, Norway, in May 2003. To simulate a large CO_2 gradient, we installed nine partly submerged mesocosms (ca. 20 m^3, 9.5 m water depth) with three different CO_2 levels and three replicates each. Due to limitations in time and resources, only one mesocosm of each treatment was sampled for analyses of dissolved amino acids and bacterial parameters. All other mesocosms served as indirect controls to compare phytoplankton bloom development and dynamics of organic matter among the different pCO_2 treatments.

The setup of the experimental system was designed by the Institute for Environmental Process Engineering (IUV, Bremen). In brief, rotary vane compressors (Becker, DT-4.8) were used to aerate the water and fumigate the gas-tight tents (95% light transmission) with air either enriched with pure CO_2 (pureness 2.7), natural air, or air depleted in CO_2. The achieved pCO_2 levels in the three treatments corresponded to 190 ppmV (past mesocosm), 370 ppmV (present mesocosm), and 700 ppmV (future mesocosm) atmospheric pCO_2 levels. In each mesocosm, seawater pCO_2 was monitored on-line, whereas pH was monitored on-line in only one of the mesocosms and less frequently in the others. The pH was maintained by running natural air through a CO_2 absorber (Na_2CO_3 platelets with a pH indicator). After 3–4 d of CO_2 adjustment, the desired pCO_2 levels in water were reached (day 0) and the CO_2 aeration of the water column was stopped. Throughout the study, the whole water column was gently mixed with an airlift using the same air as for gassing the tents. The gassing of the tents was continued to keep the pCO_2 of the overlying atmosphere at a constant level. For further details see Engel et al. (2005).

To initiate the development of a diatom bloom, 9 μmol L^{-1} NO_3, 0.5 μmol L^{-1} PO_4, and 12 μmol L^{-1} $Si(OH)_4$ were added to unfiltered, nutrient-poor, post–spring bloom seawater from the fjord on days 0 and 7 of the experiment. The upper 4 m of water column were separated from the lower part (>5 m) of the mesocosm by an artificially induced salinity gradient. In all tanks the salinity of the upper 4 m was ca. 30 and reached up to 34.2 below 5 m depth. Integrated water samples of the upper 4 m of the water column were taken by using 4 m long polyethylene tubes (10 cm in diameter), which were sealed with rubber stoppers. The samples were then transferred into 20-L carboys and immediately brought to the laboratory.

Chlorophyll a—For chlorophyll analysis, 100 mL of seawater was filtered on 0.45 cellulose nitrate filters in duplicate and immediately extracted in 90% acetone at 4°C overnight. Chlorophyll *a* (Chl *a*) concentration was measured by using a Turner Design Fluorometer (model 10-AU) and a standard solution of pure Chl *a* for calibration. Standard deviation of the duplicate measurements were usually <10%.

Amino acids—Ten-milliliter subsamples were filtered through 0.22 μm low protein binding syringe acrodisc filters

(Pall Corporation) and stored frozen at −20°C until further analysis of amino acids by high-performance liquid chromatography (HPLC). Concentrations of dissolved free amino acids (DFAA) were analyzed by HPLC after ortho-phthaldialdehyde derivatization. Dissolved combined amino acids (DCAA) were hydrolyzed with 6 mol L^{-1} HCl at 155°C for 1 h and analyzed as DFAA.

Bacterial numbers and cell size—For enumeration of free and particle-associated bacteria, 1 or 5 mL of seawater were filtered onto black 0.2 and 5.0 μm pore size Nuclepore membranes, respectively. The filters were stained with DAPI (4′6′diamidino-2-phenolindole) and stored frozen at −20°C until counting. Filters were counter-stained with 0.1% acridine orange to reduce the background fluorescence of inorganic matter. Bacteria were counted by epifluorescence microscopy (Axioplan, Zeiss, Germany) at ×1,000 magnification. The number of free bacteria was calculated by subtracting the number of particle-associated bacteria (5.0 μm filters) from that of total bacteria (0.2 μm filters). Cell sizes of free and attached bacteria were microscopically determined by using a calibrated imaging analysis system with an automated sizing function (analySIS, Germany). Bacterial cell volume was calculated from the cell's area assuming either a coccoid or rod shape.

Bacterial production and growth—Rates of bacterial protein production (BPP) were determined by incorporation of ^{14}[C]-leucine (^{14}C-Leu; Simon and Azam 1989) and bacterial cell multiplication (BCM) by incorporation of ^{3}[H]-thymidine (^{3}H-TdR; Fuhrman and Azam 1982). Both parameters were simultaneously measured in a dual label approach. Triplicates and a formalin-killed control were incubated with ^{14}C-Leu (1.15×10^{10} Bq $mmol^{-1}$; Amersham) and ^{3}H-TdR (277.5×10^{10} Bq $mmol^{-1}$; Amersham) at a final concentration of 50 nmol L^{-1}, which ensured saturation of uptake systems of both free and particle-associated bacteria. Incubation was performed in the dark at in situ temperature for 1 h. After fixation with 2% formalin, samples were filtered onto 5.0 μm (attached) and 0.2 μm (total isotope incorporation) nitrocellulose filters (Sartorius) and extracted with ice-cold 5% trichloroacetic acid (TCA) for 5 min. Thereafter, filters were rinsed twice with ice-cold 5% TCA, dissolved with ethyl acetate, and radio-assayed by liquid scintillation counting. Standard deviation of triplicate measurements was usually <15%. BPP of free bacteria was calculated by subtraction of attached BPP from total BPP. The amount of incorporated ^{14}C-Leu was converted in BPP by using an intracellular isotope dilution factor of 2. A conversion factor of 0.86 was used to convert the protein produced into carbon (Simon and Azam 1989). BCM and growth rates (μ) were calculated from ^{3}H-TdR incubations, assuming an isotope dilution factor of four and a conversion factor of 2×10^{18} cells mol^{-1} ^{3}H-TdR (Simon 1990). Whereas the BCM is a direct measurement of the cell proliferation, μ can be either calculated from BPP or BCM assuming exponential bacterial growth. Net growth rates (μ_n) were calculated from changes in total bacterial numbers during initial bacterial increase (days 0–8), decline (days 8–12), and late growth (days 12–20). The specific mortality (or loss) rate was calculated from the difference between average μ and μ_n for each growth phase.

Hydrolytic ectoenzyme activities—Aminopeptidase, α- and β-glucosidase activities were measured using L-leucine-methyl coumarinyl amide (Leu-MCA) and methyl-umbelliferyl-α- and β-D-glucoside (α-, β-D-Gluc-MUF) as substrate analogues. For each substrate, three samples and a formalin-killed control were incubated at in situ temperature in the dark for ca. 1 h. Final concentrations of substrate analogues were 100 μmol L^{-1}, which ensured maximum hydrolysis as determined by saturation kinetics. Fluorescence of both fluorochromes was measured in a TD 700 fluorometer (Turner Design) using filters ranging from 300 to 400 nm (excitation) and 410 to 610 nm (emission).

Statistical analyses—Statistical analyses were done by post hoc standard least square contrast analyses after analysis of covariance (ANCOVA) with time as the covariate and pCO_2 as the nominal predictor. Tanks 1, 4, and 7 were equivalent to future, present, and past pCO_2, respectively. Significance was given at values <0.05. We have also separately performed the same statistical analyses for the exponential phase (days 0–12) and the decline (days 14–20) of the algal bloom. Since we only had four time points for the postbloom but seven for the exponential phase of the bloom, the resulting significance levels for all measurements in the postbloom are rather uncertain. However, levels of significance only increased for numbers of free and attached bacteria in the postbloom and, hence, are given separately.

Using linear regression analysis, μ_n was calculated from changes in total bacterial numbers. Differences in regression lines of the treatments in each phase were tested for significance using comparison of slopes (interaction terms of ANCOVA). All statistical analyses were performed with the software JMP 4.02 (SAS Institute Inc.).

Results

Bloom development—The addition of inorganic nutrients to natural fjord water on day 0 led to the development of a pronounced algal bloom, which reached its maximum between days 12 and 13 of the experiment (Fig. 1a–c). Peak concentrations of Chl *a* reached 3.3 μg Chl *a* L^{-1} in the future, 4.2 μg Chl *a* L^{-1}in the present, and 3.6 μg Chl *a* L^{-1} in the past mesocosm. In addition to Chl *a*, substantial differences in algal species composition were observed within different CO_2 treatments (Martin-Jézéquel et al. pers. comm.). Coccolithophorids (mainly *Emiliania huxleyi*) developed first in the future mesocosm, followed by diatoms, which reached almost equal numbers from day 15 on. In contrast, the present mesocosm was almost exclusively dominated by coccolithophorids. In the past mesocosm, coccolithophorids and diatoms contributed to equal proportions until day 15, but thereafter coccolithophorids became increasingly dominant. Phytoplankton bloom development led to a constant decrease of nitrate and phosphate, which reached their detection limit in all mesocosms at maximum Chl *a* values on days 12 and 13 (U. Riebesell unpubl. data). Whereas concentrations of particulate organic carbon (POC)

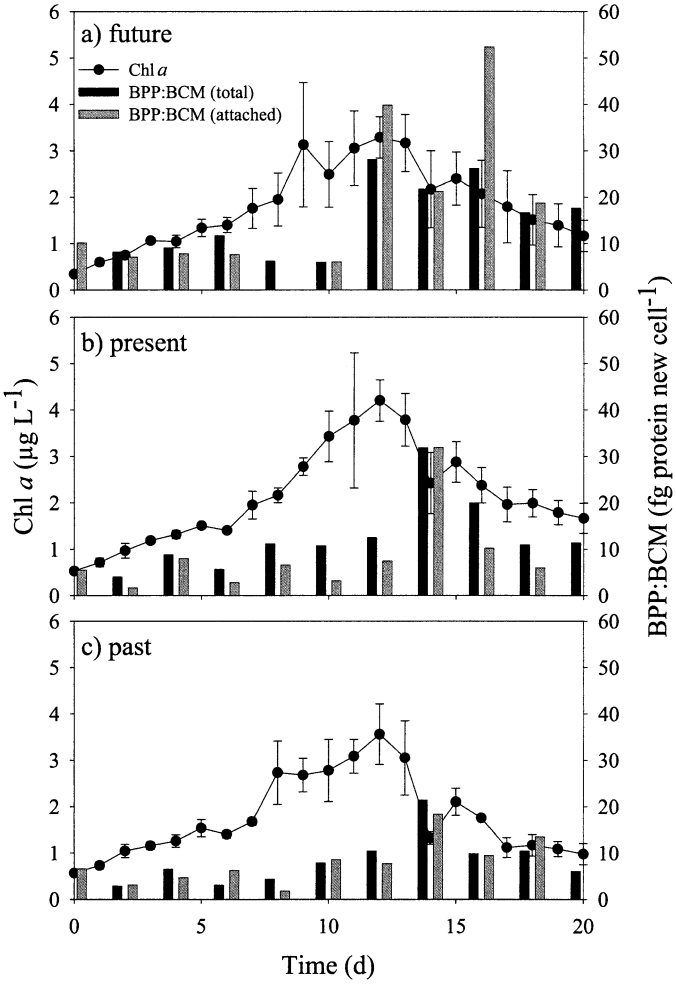

Fig. 1. Concentration of Chl *a* and BPP : BCM ratio of total as well as attached bacteria in (a) future, (b) present, and (c) past mesocosms. For further explanation see text.

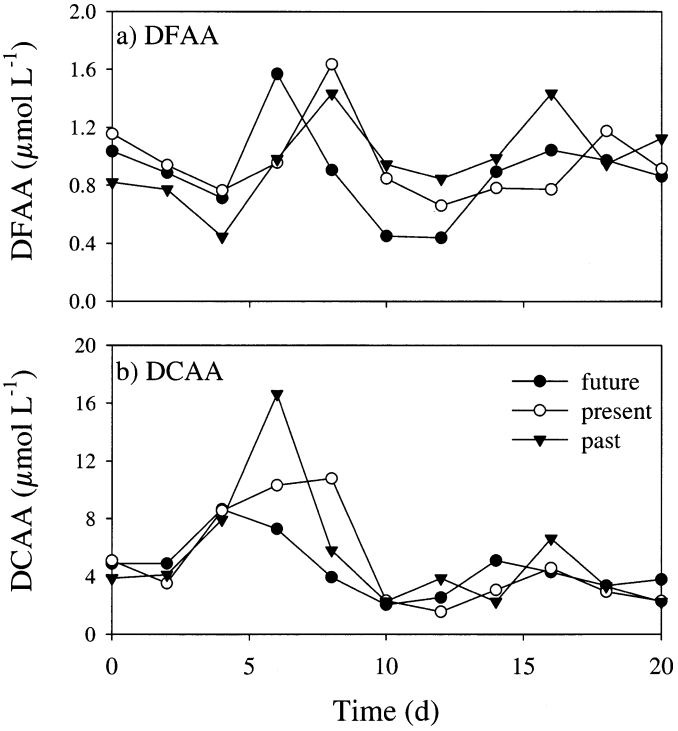

Fig. 2. Concentrations of (a) dissolved free (DFAA) and (b) dissolved combined amino acids (DCAA) in mesocosms with future, present, and past CO_2 concentrations. Standard deviations of triple measurements were <10%.

and algal numbers were significantly correlated throughout the whole experiment, those of POC and Chl *a* were only correlated until day 12. The better correlation between POC and algal number during the declining phase of the bloom indicates changes in algal physiology and formation of detrital matter. Concentrations of DOC remained almost constant at about 100 μmol L^{-1} in all mesocosms throughout the experiment and reflected neither phytoplankton nor POC development. The comparison between replicate mesocosms revealed that chemical and biological parameters of our selected mesocosms (mesocosms 1, 4, and 7) were in line with the replicates of each CO_2 treatment and did not include outliers (U. Riebesell unpubl. data). Hence we are confident that our results obtained from only one mesocosm of each treatment are representative for the respective pCO_2 level.

Amino acids—Concentrations of DFAA and DCAA ranged between 0.4 and 1.6 μmol L^{-1} and 2 and 17 μmol L^{-1}, respectively (Fig. 2a,b). The first peak in DFAA concentrations occurred between days 6 and 8 and reached similar concentrations in all three mesocosms. The second, less pronounced peak on days 16–18 was highest in the past and lowest in the future mesocosm (Fig. 2a). Concentrations of DCAA were more variable between the mesocosms and with time than those of DFAA. Maxima of DCAA occurred in the future mesocosm on day 4 (8.5 μmol L^{-1}), in the present mesocosm on day 8 (10 μmol L^{-1}), and in the past mesocosm on day 6 (17 μmol L^{-1}; Fig. 2*b*). Differences in DFAA or DCAA concentrations between treatments were not statistically significant, except that DCAA concentration in the future mesocosm was significantly lower than that in the past mesocosm (Table 1). This statistical difference was, however, mainly the result of one data point; the peak concentration of DCAA during the first maxima was very high in the past mesocosm (Fig. 2b).

Bacterial numbers—Numbers of total and free bacteria were similar in all mesocosms during the whole study period, whereas numbers of attached bacteria were significantly higher in the future mesocosm (Fig. 3; Table 1). However, both concentrations of free ($p < 0.0001$, $n = 4$) and attached bacteria ($p = 0.0001$, $n = 4$) were significantly dependent on pCO_2 during the decline of the algal bloom (days 14–20).

Highest numbers of total as well as free bacteria were recorded between days 6 and 8. The peaks in numbers of total and free bacteria on days 6 and 8 were paralleled by those of DFAA and DCAA. Abundance of total and free bacteria dramatically decreased when Chl *a* strongly increased between days 8 and 12. Thereafter, numbers of total and free bacteria slowly increased during the breakdown of

Table 1. Statistical analyses using post hoc analyses after ANCOVA with time as the covariate and pCO_2 as the nominal predictor. All statistical analyses were performed with the software JMP 4.02. Mesocosms 1, 4, and 7 are equivalent to future, present, and past pCO_2, respectively.

Mesocosms	DFAA	DCAA	Free bacteria	Attached bacteria	BPP_{tot}	BPP_{att}	cs BPP_{tot}	cs BPP_{att}	BCM_{tot}	BCM_{att}	μ_{tot}
Variables											
1 vs. 4	NS	NS	NS	0.0034	0.0077	0.0021	0.0436	0.0012	0.0327	0.009	0.0265
4 vs. 7	NS	NS	NS	NS	NS	NS	NS	NS	0.0248	NS	0.0257
1 vs. 7	NS	0.0483	NS	0.0004	0.0281	0.0039	0.0770	0.0026	NS	0.03	NS
Whole model of variance	NS	NS	<0.001	<0.001	0.0005	0.0019	0.0009	0.0046	0.0499	0.0327	NS
pCO_2 (nominal predictor)	NS	NS	NS	NS	0.0181	0.0036	NS	0.0017	0.0417	0.0307	0.03

NS, not significant; cs, cell-specific; tot, total; att, attached.

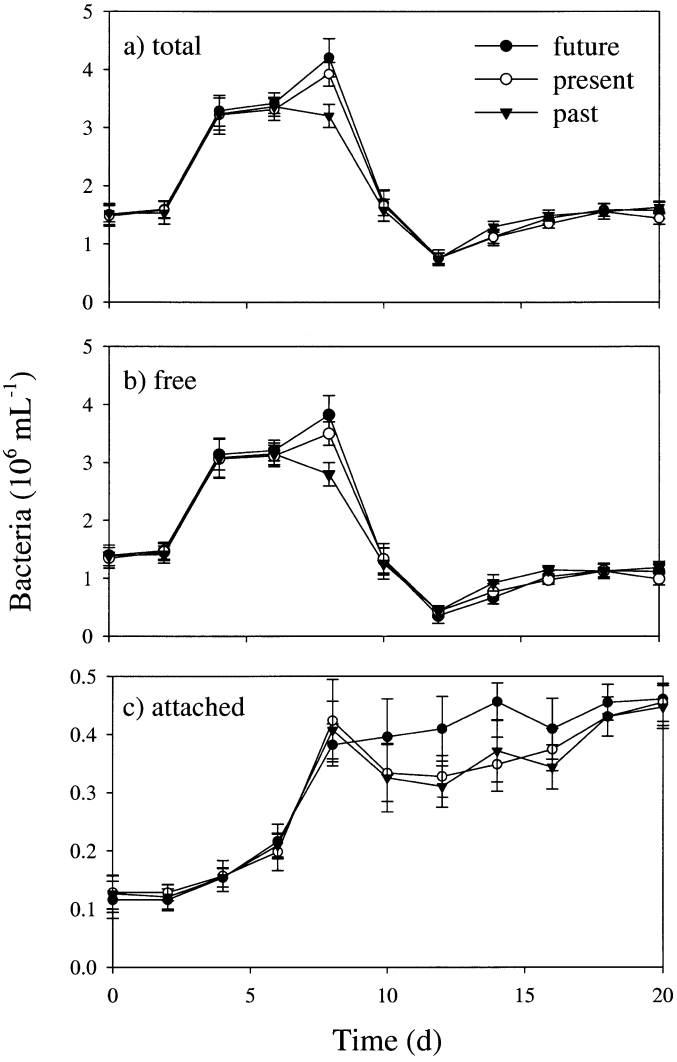

Fig. 3. Abundances of (a) total, (b) free, and (c) particle-associated bacteria in mesocosms with future, present, and past CO_2 concentrations. Standard deviations are given for 10 counting fields.

the algal bloom (Fig. 3a,b) when DFAA concentrations were slightly enhanced. In contrast, concentrations of attached bacteria increased rapidly until day 8 and further increased at a slower rate during the peak and breakdown of the algal bloom. Numbers of attached bacteria were appreciably higher in the future mesocosm compared with the other mesocosms after day 8 (Fig. 3c; Table 1). Lowest numbers of total and free bacteria occurred on day 12 in all mesocosms, when Chl *a* concentration was highest and that of DFAA and DCAA relatively low. At this time the fraction of attached bacteria was highest, reaching ca. 40% in the past and present mesocosms and ca. 50% in the future mesocosm. Thereafter, the abundance of attached bacteria increased slower than that of free bacteria, resulting in decreasing percentages of attached bacteria during the decline of the algal bloom. In general, bacterial numbers remained relatively low during the algal bloom and its decline.

Bacterial sizes—Sizes of free bacteria ranged between 0.04 and 0.2 μm^3, with larger bacteria common during the peak and decline of the algal bloom (days 12–18). Attached bacteria were significantly bigger and increased from 0.6 to 1.5 μm^3 at the end of the experiment. Attached bacteria contributed to 40%–80% of the total bacterial volume.

Total and cell-specific bacterial protein production—BPP of free living bacteria was similar in all mesocosms and showed little temporal variability, with only a slight increase during the declining phase of the bloom. Total BPP as well as BPP of attached bacteria showed a pronounced temporal pattern with lowest values during the height of the algal bloom. Both were significantly higher in the future mesocosm (Table 1). Total BPP ranged between 0.8 and 11.8 $\mu g\ C\ L^{-1}\ h^{-1}$, with a small BPP peak in the future mesocosm coinciding with elevated bacterial numbers and amino acids on days 4–8 (Fig. 4a). Total BPP was much higher during the decline of the algal bloom between days 14 and 18 (Fig. 4a) when POC (data not shown) was highest. During this time bacterial numbers increased only a little and concentrations of DFAA were slightly elevated. BPP of attached bacteria often surpassed that of free bacteria and comprised most of the total BPP. BPP of attached bacteria was highest

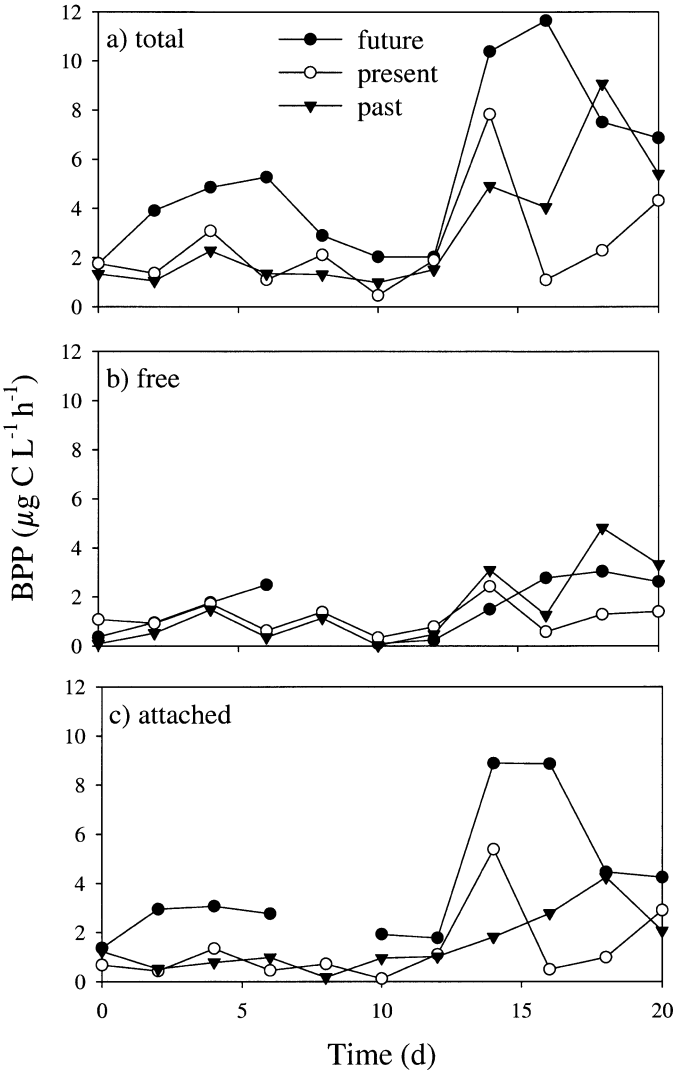

Fig. 4. Carbon production (BPP) of (a) total, (b) free, and (c) particle-associated bacteria in mesocosms with future, present, and past CO_2 concentrations. Standard deviations of triple measurements were <15%.

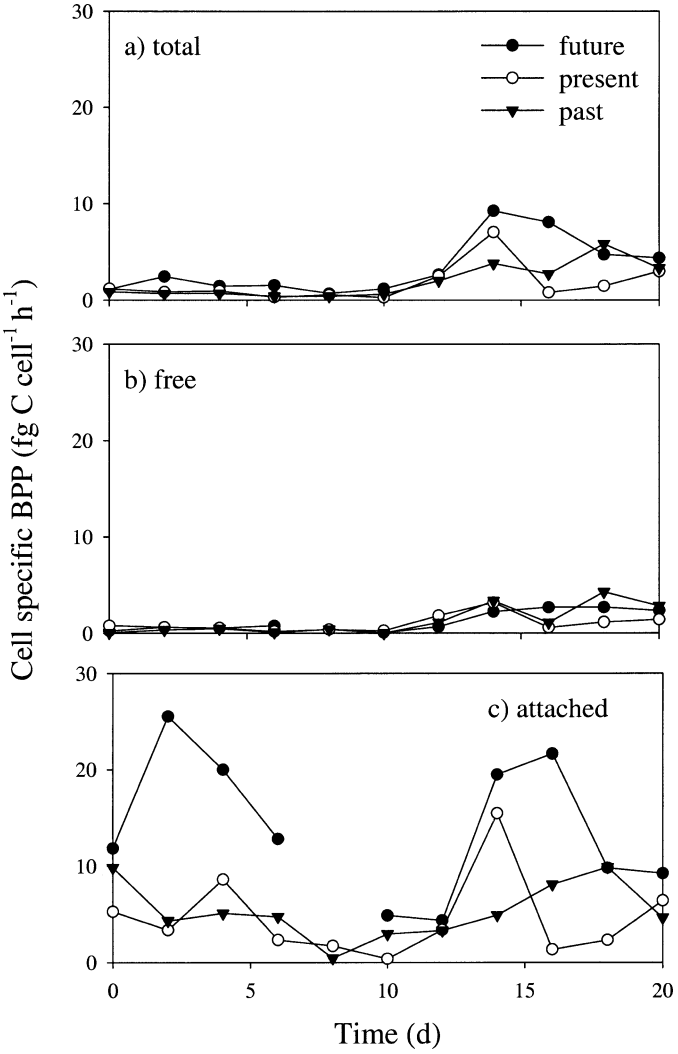

Fig. 5. Cell-specific BPP of (a) total, (b) free, and (c) particle-associated bacteria in mesocosms with future, present, and past CO_2 concentrations.

between days 14 and 16 after the peak in Chl *a*, especially in the future mesocosm (Fig. 4b,c; Table 1).

Differences in BPP between free and attached bacteria as well as between CO_2 treatments became more obvious when calculating cell-specific rates (Fig. 5; Table 1). Cell-specific BPP of all bacterial fractions was lowest during the height of the bloom. However, cell-specific BPP of total and free bacteria slightly increased during the decline of the algal bloom (Fig. 5a,b). Cell-specific BPP of attached bacteria differed between mesocosms, with highest rates (up to 25.5 fg cell^{-1} h^{-1}) in the future mesocosm already on the second day of the experiment. In the same mesocosm, cell-specific BPP of attached bacteria was also high during the decline of the algal bloom (up to 21.6 fg cell^{-1} h^{-1}; Fig. 5c; Table 1).

Bacterial cell multiplication and growth rate—In general, total BCM and μ were similar to total BPP with two maxima, one on days 2–6 and the second during the declining phase of the algal bloom (Figs. 6a and 7a). Both total BCM and total μ depended slightly but significantly on the pCO_2 treatment, with lower values in the present mesocosm (Table 1). BCM and μ of free bacteria were lowest on days 10 and 12 at the bloom peak (Figs. 6b and 7b). Thereafter, both parameters were different for each treatment and did not show any uniform temporal trend. BCM and μ of attached bacteria were higher in the future mesocosms, especially during the first 10 d of the experiment (Figs. 6b and 7b). Minimum values were observed in all mesocosms during the bloom peak, just as for free bacteria. Differences in BCM and μ between attached and free bacteria were less pronounced than in BPP.

BPP : BCM ratio—The BPP : BCM ratio is a good indication for bacterial growth characteristics (i.e., the amount of protein produced per new cell; Simon 1990). Ratios were high for total and attached bacteria at the peak of the algal

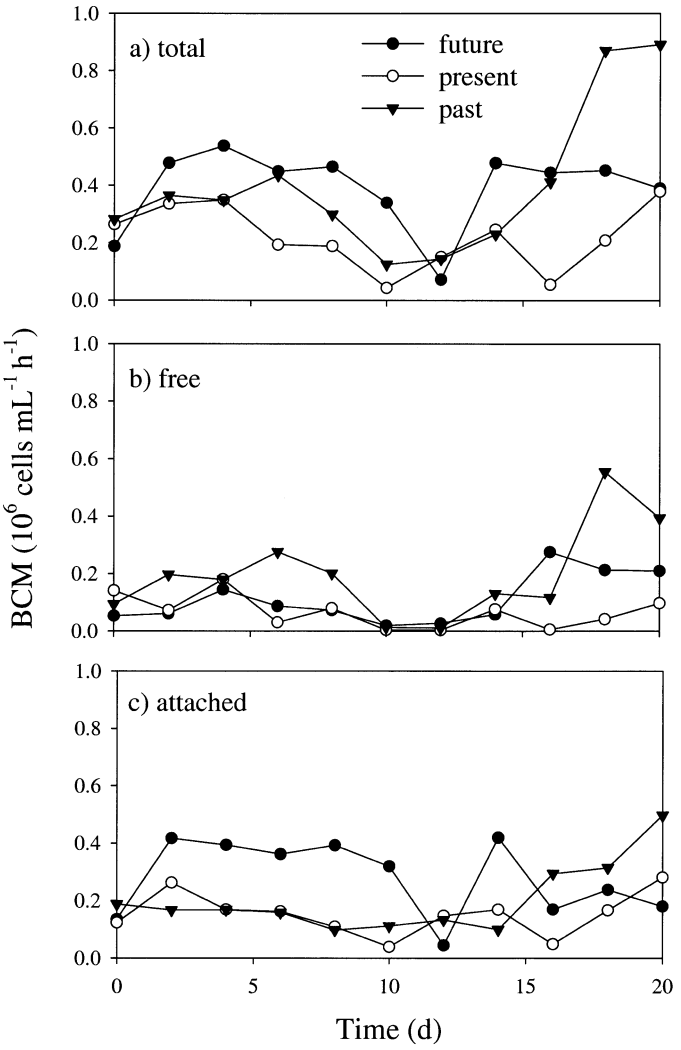

Fig. 6. Bacterial cell multiplication rate (BCM) of (a) total, (b) free, and (c) particle-associated bacteria in mesocosms with future, present, and past CO_2 concentrations. Standard deviations of triple measurements were <15%.

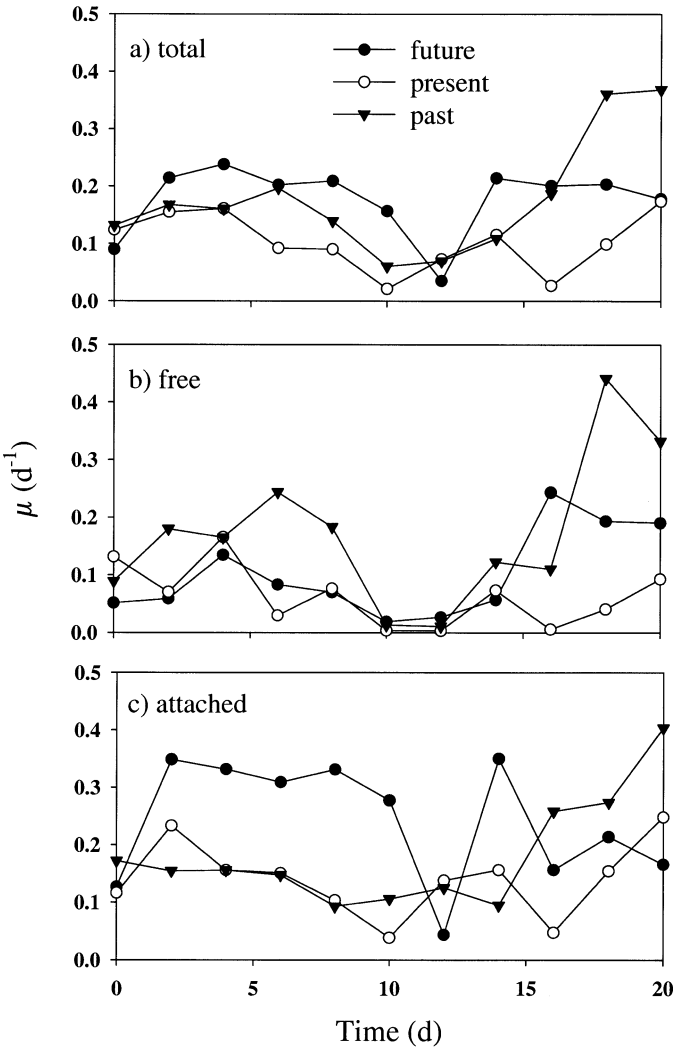

Fig. 7. Bacterial growth rate (μ) of (a) total, (b) free, and (c) particle-associated bacteria in mesocosms with future, present, and past CO_2 concentrations.

bloom (future mesocosm) and during the breakdown of the bloom (Fig. 1a–c). Highest values of 52 fg protein new $cell^{-1}$ were measured on day 16 for attached bacteria in the future mesocosm. They were also high on day 14 in the present (31 fg protein new $cell^{-1}$), but much lower in the past mesocosm (19 fg protein new $cell^{-1}$).

Hydrolytic ectoenzyme activities—Protease activity was significantly higher in the future mesocosm compared with protease activity in the present and past mesocosms (Fig. 8a; Table 2). Peaks in protease activity, especially in the future mesocosm, paralleled that of DFAA on day 6 and that of the algal bloom (Chl *a*) on day 12 (Fig. 8a). Cell-specific protease activity was also significantly higher in the future mesocosm compared with the present and past mesocosms (Table 2).

The activity of α-glucosidase in the future mesocosm was significantly higher than in the past mesocosm but did not differ statistically from that in the present mesocosm (Table 2). Peaks in α-glucosidase activity, especially in the future mesocosm, paralleled that of DFAA on day 6 and that of the algal bloom (Chl *a*) on day 12 (Fig. 8b). Cell-specific α-glucosidase activity showed only one peak in parallel to Chl *a* and was highest in the future mesocosm. Differences between mesocosms were not statistically significant (Table 2).

Similar to α-glucosidase, total and cell-specific activities of β-glucosidase were highest during the peak of the algal bloom (Fig. 8c) and in the future mesocosm, but neither total nor cell-specific β-glucosidase activities differed significantly with pCO_2 (Table 2).

Discussion

The recent and projected increase in oceanic pCO_2 may have profound consequences for oceanic phytoplankton communities and particle dynamics (Tortell et al. 2002; Zondervan et al. 2002; Engel et al. 2005). Since marine heterotrophic bacteria play a major role in nutrient and organic

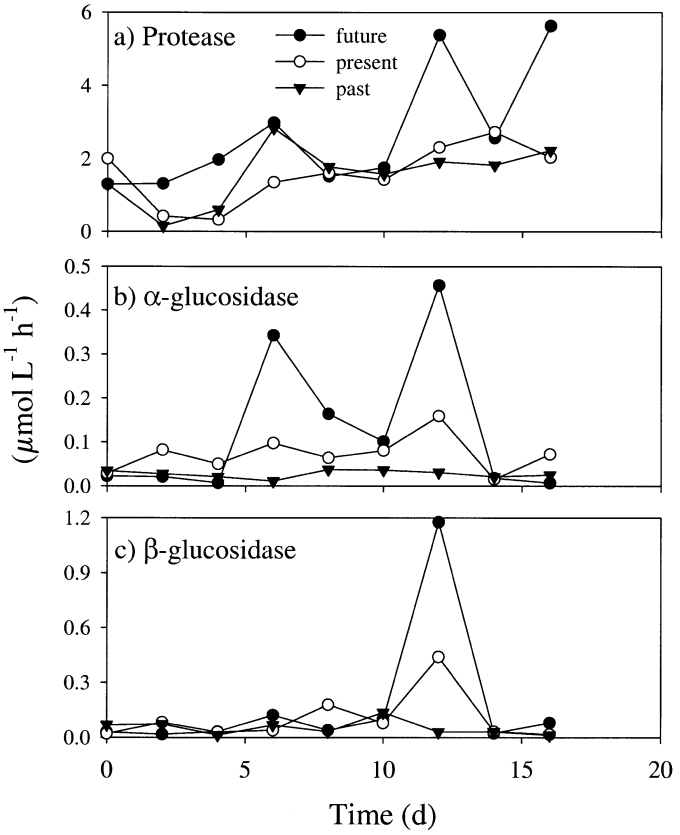

Fig. 8. Hydrolytic activities of (a) protease, (b) α-glucosidase, and (c) β-glucosidase in mesocosms with future, present, and past CO_2 concentrations. Standard deviations of triple measurements were <10%.

matter cycling (Azam 1998), it is important to know whether changes in oceanic pCO_2 will also affect the dynamics of the bacterioplankton in the sea. We used an experimental setup that allowed us to establish and maintain different atmospheric pCO_2 levels in large outdoor mesocosms containing a natural plankton assemblage in order to investigate the impact of pCO_2 on bacterioplankton dynamics during the development and decline of phytoplankton blooms.

Temporal dynamics—Concentrations of DOC did not change over time, whereas both DFAA and DCAA showed a pronounced temporal pattern, which was similar for all treatments. This suggests that the composition of dissolved organic matter (DOM) may have substantially changed over time. Although algal concentrations were still low, the highest peaks in DCAA occurred between days 4 and 8 and were accompanied or followed by those in DFAA. The coinciding peak in protease activity may indicate that DFAA were hydrolysis products of DCAA degradation (Grossart and Simon 1998). At the same time, numbers of free bacteria, BCM, and μ increased as well. It is possible that elevated concentrations of DFAA and DCAA were the result of protein release by phytoplankton due to lysis or grazing.

The abundance of bacteria was relatively low both at the peak of the algal bloom and during its breakdown. Low numbers of bacteria and low bacterial activities at the height of the algal bloom may also be induced by antibacterial activities of the algae. Many algae species, including *E. huxleyi*, are known to produce antimicrobial substances (Wolfe et al. 1997), which effectively suppress bacterial growth. However, as *E. huxleyi* was more important in the present tank rather than the future mesocosm, and as the bacterial numbers exhibited a steep decline, this mechanism cannot easily account for the observed differences.

A comparison between μ, calculated from BCM (gross growth rate) and μ_n, estimated from changes in cell concentration, indicates times during which loss processes were high. Whereas μ was relatively constant during the whole experiment with an average value of 0.18 d^{-1}, estimated μ_n is best divided into three phases: (1) the initial rapid growth up to day 8, (2) the rapid decline between days 8 and 12, and (3) the final growth period after day 12. In the future mesocosm, μ_n was 0.36, −0.86 (net loss), and 0.14 d^{-1} during all three phases, respectively (Table 3). For each growth phase, μ_n of total bacteria between the different mesocosms were statistically tested and showed significant differences in phase 1 (future vs. past mesocosm, $p = 0.0017$) and in phase 2 (future vs. past, $p < 0.0001$, and present vs. past, $p = 0.0012$). All other tests were not significant.

During the initial growth phase, the difference between μ and μ_n was rather small and may easily be explained by

Table 2. Statistical analyses using post hoc analyses after ANCOVA with time as the covariate and pCO_2 as the nominal predictor. All statistical analyses were performed with the software JMP 4.02. Mesocosms 1, 4, and 7 are equivalent to future, present, and past pCO_2, respectively.

Mesocosms	Protease activity	cs protease activity	α-glucosidase	cs α-glucosidase	β-glucosidase	cs β-glucosidase
Variables						
1 vs. 4	0.0174	0.0084	NS	NS	NS	NS
4 vs. 7	NS	NS	NS	NS	NS	NS
1 vs. 7	0.0174	0.0318	0.0468	NS	NS	NS
Whole model of variance	<0.0019	0.033	NS	NS	NS	NS
pCO_2 (nominal predictor)	0.0211	0.0188	NS	NS	NS	NS

cs, cell-specific; NS, not significant.

Table 3. Net growth rates (μ_n) calculated from the change in total bacterial numbers during initial bacterial increase (days 0–8), decline (days 8–12), and late growth (days 12–20). R^2 values are given for linear regression analysis.

	Future		Present		Past	
Days	μ_n (d^{-1})	R^2	μ_n (d^{-1})	R^2	μ_n (d^{-1})	R^2
0–8	0.36	0.91	0.33	0.90	0.26	0.74
8–12	−0.86	0.94	−0.79	0.94	−0.61	0.97
12–20	0.14	0.88	0.09	0.82	0.10	0.81

grazing of nanoflagellates and protozooplankton, which in turn were presumably controlled by their predators. The sudden steep decrease in μ_n at a time when μ decreased much less suggests a sudden destructive event such as a viral infection. Viral numbers strongly increased and reached their maximum shortly after the first peak in bacterial numbers on day 11 (Mühling et al. unpubl. data). Thereafter, viral numbers remained high when bacterial numbers were extremely low at the peak of the algal bloom. In addition, high aggregation and presumably increased sedimentation rates in the future mesocosm (U. Riebesell unpubl. data) may have also contributed to higher loss rates in this tank, resulting in similar bacterial numbers in all tanks during the development and decline of the phytoplankton bloom, although bacterial activity in the future mesocosm was higher.

During the final phase of the experiment, bacterial numbers only very slowly increased, although the gross growth rate μ was slightly higher than it was initially and organic matter concentrations were high. During this period the BPP : BCM ratio was relatively high in all mesocosms (Fig. 1a–c), indicating a changed physiology and biomass of the newly formed cells relative to earlier. It is possible that virus infections were still reducing bacterial concentrations and grazing pressure on the larger cells may have been heavier at this time. Increased cell sizes of bacteria as well as aggregated and/or attached bacteria provide food for additional predators (Kiørboe et al. 2004), which require larger food particles.

pCO_2 related effects on bacterial dynamics—During this study we measured bacterial abundance, production, growth rate, and hydrolytic ectoenzyme activities of both free and particle-associated bacteria to better resolve effects of different pCO_2 on bacterioplankton dynamics. Significantly higher values as a function of pCO_2 were observed for total BPP, protease activity, and cell-specific protease activity as well as for BPP, cell-specific BPP, BCM, and μ of attached bacteria (Tables 1 and 2). Although statistically not significant, appreciably higher average rates in the future mesocosm were also observed for α- and β-glucosidase activity as well as for the respective cell-specific activities. It may be concluded that during our experiment concentrations and activities of attached bacteria as well as all determined hydrolytic ectoenzyme activities were appreciably higher in the mesocosm, thus mimicking future pCO_2 conditions compared with the other mesocosms.

Total bacterial concentrations were dominated by free bacteria, whereas total BPP was dominated by attached bacteria. Although numbers of attached bacteria were also significantly higher in the future mesocosm relative to the present and past mesocosms, statistical analysis indicated that time, rather than pCO_2, was responsible for that pattern (Table 1). Significant differences in the concentration of both free and attached bacteria between mesocosms occurred in the second half of the study during the decline of the bloom. This indicates that differences in pCO_2 may have an increased effect on abundances of free and attached bacteria when the release of algal-derived organic matter is high during the decay of the algal bloom (Smith et al. 1995). A similar study in which smaller mesocosms have been used did not find any pCO_2-dependent differences in total bacterial numbers (Rochelle-Newall et al. 2004). These authors did not distinguish between free and attached bacteria or between different growth phases of the algae, which may account for the observed differences.

Studies on pCO_2-related effects on bacterial activities are scarce and also do not distinguish between activities of free and attached bacteria. Results of the only other available study, which investigated the impact of changes in pCO_2 onto bacterial production, were ambiguous, with changes in ambient pressure and temperature having a larger effect than those of pH (Coffin et al. 2004). If the bacterial assemblage, coming from a depth of 600 m, was repressurized, mild acidification (pH 6.95) induced by CO_2 injection appeared to enhance bacterial production, whereas bacterial production appeared to be suppressed at pH 5.6. All of these experiments were performed in darkness and do not account for changes in photosynthetic activity and, hence, availability and quality of bacterial substrates. The pH of the future mesocosm of our experiment increased from 7.8 to 8.1 due to photosynthetic activity during the bloom. The minimum pH in our experiment (7.8, 8.1, and 8.3 for future, present, and past mesocosms, respectively) was appreciably higher (less acidic) compared with that in the experiments by Coffin et al. (2004). Moreover, experiments by Coffin et al. (2004) were performed with bacterial communities from the deep ocean, which are distinctly different from those at the surface (Giovannoni et al. 1996). Possibly, large shifts in pH affect the integrity of bacterial cells and reduce their metabolic rates. Changes observed during the mesocosm study presented here were observed on the timescale of days to weeks, rather than hours to days. In our experiments, a continuous supply of labile bacterial substrates, such as proteins and carbohydrates, may have prolonged the effect of rising CO_2 concentrations due to increased photosynthetic release. Bacteria in the experiment of Coffin et al. (2004) were presumably limited in labile bacterial substrates after 70 h of incubation. This suggests that a continuous supply of labile organic matter is necessary to sustain the positive effect of high pCO_2 on bacterial activities. For example, the amount and quality of phytoplankton-derived organic matter significantly differ with pCO_2 (Engel et al. 2004, 2005).

In laboratory experiments with natural phytoplankton, the formation of TEP, which form from phytoplankton exudates, was increased at elevated pCO_2 concentrations (Engel 2002), but maximal TEP concentrations were observed at pCO_2 concentrations not much higher than ambient. Possibly, a

lack of adaptation of the algal cells to higher pCO_2 concentrations resulted in the lack of a further increase in the TEP production at higher than ambient pCO_2 concentrations during that investigation. During a mesocosm study similar to the one we describe here, the production of TEP normalized to cell abundance of the dominating autotroph and *E. huxleyi* was highest in the future treatment (Engel et al. 2004). An increased production of TEP, which would provide surfaces for bacteria (Passow and Alldredge 1994) and promote aggregation (Passow et al. 1994), would favor attached bacteria. It has long been known that fresh phytoplankton exudates and the formation of particles from fresh exudates stimulates activities and growth of attached bacteria (e.g., Johnson and Cooke, 1980). Bacteria associated with aggregates also exhibit higher activity levels and ectoenzyme production compared with free bacteria (Smith et al. 1995; Grossart and Ploug 2001). In our study, the positive relationship between enzyme activity and pCO_2 was especially strong for protease activity, which is mainly generated by particle-bound bacteria (Simon et al. 2002, and references therein).

The development of the phytoplankton community composition was different in the different pCO_2 treatments (Martin-Jézéquel et al. pers. comm.). For example, the future mesocosm was initially dominated by the coccolithophorids, whereas the proportion of diatoms strongly increased in the later stage of the bloom. Changes in phytoplankton composition also led to changes in bacterial community structure (Pinhassi et al. 2004; Grossart et al. 2005) and subsequently in bacterial activities (Riemann et al. 2000). Comparison of the bacterial community in our mesocosms using denaturing gradient gel electrophoresis (DGGE) of PCR-amplified 16S rRNA gene segments, however, revealed only minor differences in bacterial community structure with pCO_2 and over time (Mühling et al. unpubl. data). The observed minor differences may be partly due to the fact that Mühling et al. did not distinguish between free and attached bacteria and that they have solely used eubacterial PCR primers, which may limit the resolution of specific bacteria. To our knowledge there is no study that has yet addressed the bacterial community attached to *E. huxleyi*. However, from our studies on bacteria attached to diatoms, we know that the bacterial community structure dramatically changes with the physiological status of the alga (Grossart et al. 2005). For the diatom *Thalassiosira rotula*, we also found significant changes in the role of bacteria for organic matter utilization and aggregation processes (H.-P. Grossart unpubl. data). Furthermore, quantity and quality of phytoplankton-derived dissolved and particulate matter greatly differs among coccolithophorids (*E. huxleyi*) and diatoms (*Skeletonema costatum*; Biersmith and Benner 1998). In addition to the alga's physiology, changes in phytoplankton community structure in the different pCO_2 treatments differed over time and, hence, quantity and quality of phytoplankton-derived organic matter may have been highly variable over time. A recent study (Engel et al. 2004) shows that aggregation of dissolved polysaccharides derived from *E. huxleyi* can act as a potential sink of DOC. Similar changes in particle dynamics may have occurred in our study and suggest an impact predominately on concentrations and activities of attached bacteria (see above). Phytoplankton exudates and subsequent aggregate formation have a significant impact on attached bacteria (e.g., Smith et al. 1995). A higher rate of exudation at lower primary production could be the direct result of elevated atmospheric CO_2 concentrations or could at least in part be the consequence of the different phytoplankton community composition.

Throughout the whole study, BPP of especially attached bacteria and protease activity differed significantly as a function of pCO_2. In addition, numbers of free and attached bacteria depended on pCO_2, but only at the decline of the algal bloom. Through separation of free and attached bacteria by means of differential filtration we could demonstrate that the increase in bacterial activity at higher pCO_2 was mainly due to activities of attached bacteria. The relationship between pCO_2 and activity of attached bacteria is most likely an indirect one caused by pCO_2-induced changes in photosynthetic production of dissolved and particulate organic matter. Our study reveals evidence that pCO_2-induced shifts in particle quality (Engel et al. 2005) and particle dynamics (Engel et al. 2004) affect bacterial activities and, hence, organic matter cycling and sinking flux. Under realistic global change scenarios, increasing seawater CO_2 concentrations will go hand in hand with rising surface ocean temperatures, increased stratification, and decreasing nutrient supply to the surface layer. These environmental changes may compensate or amplify direct effects of increasing CO_2 levels and the related changes in seawater chemistry. To predict the effect of changing pCO_2 on bacterial dynamics and organic matter cycling in the sea, we need to broaden the focus by including the combined effects of all projected changes in environmental conditions.

References

ARMSTRONG, R. A., C. LEE, J. I. HEDGES, S. HONJO, AND S. G. WAKEHAM. 2002. A new, mechanistic model for organic carbon fluxes in the ocean based on the quantitative association of POC with ballast minerals. Deep-Sea Res. II **49:** 219–236.

AZAM, F. 1998. Microbial control of oceanic carbon flux: The plot thickens. Science **280:** 694–696.

BIERSMITH, A., AND R. BENNER. 1998. Carbohydrates in phytoplankton and freshly produced dissolved organic matter. Mar. Chem. **63:** 131–144.

BIJMA, J., H. J. SPERO, AND D. W. LEA. 1999. Reassessing foraminiferal stable isotope geochemistry: Impact of the oceanic carbonate system (experimental results), p. 489–512. *In* G. Fisher and G. Wefer [eds.], Use of proxies in paleooceanography: examples from the South Atlantic. Springer-Verlag.

BURKHARDT, S., G. AMOROSO, U. RIEBESELL, AND D. SULTEMEYER. 2001. CO_2 and HCO_3-uptake in marine diatoms acclimated to different CO_2 concentrations. Limnol. Oceanogr. **46:** 1378–1391.

CALDEIRA, K., AND M. E. WICKETT. 2003. Anthropogenic carbon and ocean pH. Nature **425:** 365.

COFFIN, R. B., M. T. MONTGOMERY, T. J. BOYD, AND S. M. MASUTANI. 2004. Influence of ocean CO_2 sequestration on bacterial production. Energy **29:** 1511–1520.

COLE, J. J., S. FINDLAY, AND M. L. PACE. 1988. Bacterial production in fresh and saltwater: A cross-system overview. Mar. Ecol. Progr. Ser. **43:** 1–10.

ENGEL, A. 2002. Direct relationship between CO_2 uptake and trans-

parent exopolymer particle production in natural phytoplankton. J. Plankton Res. **24:** 49–53.

———, B. DELILLE, S. JACQUET, U. RIEBESELL, E. ROCHELLE-NEWALL, A. TERBRÜGGEN, AND I. ZONDERVAN. 2004. Transparent exopolymer particles and dissolved organic carbon production by *Emiliania huxleyi* exposed to different CO_2 concentrations: A mesocosm experiment. Aquat. Microb. Ecol. **34:** 93–104.

———, AND U. PASSOW. 2001. Carbon and nitrogen content of transparent exopolymer particles (TEP) in relation to their Alcian Blue adsorption. Mar. Ecol. Prog. Ser. **219:** 1–10.

———, AND OTHERS. 2005. Testing the direct effect of CO_2 concentration on a bloom of the coccolithophorid *Emiliania huxleyi* in mesocosm experiments. Limnol. Oceanogr. **50:** 493–507.

FUHRMAN, J. A., AND F. AZAM. 1982. Thymidine incorporation as a measure of heterotrophic bacterioplankton production in marine surface waters: Evaluation and field results. Mar. Biol. **66:** 109–120.

GIOVANNONI, S. J., M. S. RAPPE, K. L. VERGIN, AND N. L. ADAIR. 1996. 16S rRNA genes reveal stratified open ocean bacterioplankton populations related to the green non-sulfur bacteria. Proceedings of the National Academy of Sciences of the United States of America **93:** 7979–7984.

GROSSART, H. P., F. LEVOLD, M. ALLGAIER, M. SIMON, AND T. BRINKHOFF. 2005. Marine diatom species harbour distinct bacterial communities. Envir. Microbiol. **7:** 860–873.

———, AND H. PLOUG. 2001. Microbial degradation of organic carbon and nitrogen on diatom aggregates. Limnol. Oceanogr. **46:** 267–277.

———, AND M. SIMON. 1998. Bacterial colonization and microbial decomposition of limnetic organic aggregates (lake snow). Aquat. Microb. Ecol. **15:** 127–140.

HOUGHTON, J. T., Y. DING, D. J. GRIGGS, M. NOGUER, P. J. VAN DER LINDEN, X. DAI, K. MASKELL, AND C. A. JOHNSON. 2001. Climate change 2001: The scientific basis: Contribution of working group I to the third assessment report of the intergovernmental panel of climate change. Cambridge Univ. Press.

JOHNSON, B. D., AND R. C. COOKE. 1980. Organic particle and aggregate formation resulting from the dissolution of bubbles in seawater. Limnol. Oceanogr. **25:** 653–661.

KIØRBOE, T., H. P. GROSSART, H. PLOUG, K. TANG, AND B. AUER. 2004. Particle-associated flagellates: Swimming patterns, colonization rates, and grazing on attached bacteria. Aquat. Microb. Ecol. **35:** 141–152.

KLAAS, C., AND D. ARCHER. 2002. Association of sinking organic matter with various types of mineral ballast in the deep sea: Implications for the rain ratio. Global Biochem. Cycles **16:** 1–14.

MARI, X., S. BEAUVAIS, R. LEMEE, AND M. L. PEDROTTI. 2001. Non-Redfield C : N ratio of transparent exopolymeric particles in the northwestern Mediterranean Sea. Limnol. Oceanogr. **46:** 1831–1836.

PASSOW, U., AND A. L. ALLDREDGE. 1994. Distribution, size, and bacterial colonization of transparent exopolymer particles (TEP) in the ocean. Mar. Ecol. Prog. Ser. **113:** 185–198.

———, A. L. ALLDREDGE, AND B. E. LOGAN. 1994. The role of particulate carbohydrate exudates in the flocculation of diatom blooms. Deep-Sea Res. I **41:** 335–357.

PINHASSI, J., M. M. SALA, H. HAVSKUM, F. PETERS, O. GUADAYOL, A. MALITS, AND C. MARRASE. 2004. Changes in bacterioplankton composition under different phytoplankton regimens. Appl. Environ. Microbiol. **70:** 6753–6766.

RIEBESELL, U., I. ZONDERVAN, B. ROST, P. D. TORTELL, R. E. ZEEBE, AND F. M. M. MOREL. 2000. Reduced calcification in marine plankton in response to increased atmospheric CO_2. Nature **407:** 634–637.

RIEMANN, L., G. F. STEWARD, AND F. AZAM. 2000. Dynamics of bacterial community composition and activity during a mesocosm diatom bloom. Appl. Environ. Microbiol. **66:** 578–587.

ROCHELLE-NEWALL, E., B. DELILLE, M. FRANKIGNOULLE, J. P. GATTUSO, S. JAQUET, U. RIEBESELL, A. TERBRÜGGEN, AND I. ZONDERVAN. 2004. Chromophoric dissolved organic matter in experimental mesocosms maintained under different pCO_2 levels. Mar. Ecol. Prog. Ser. **272:** 25–31.

SIMON, M. 1990. Improved assessment of bacterial production: Combined measurements of protein synthesis via leucine and cell multiplication via thymidine incorporation. Arch. Hydrobiol. Beih. Ergebn. Limnol. **34:** 151–155.

———, AND F. AZAM. 1989. Protein content and protein synthesis rates of planktonic marine bacteria. Mar. Ecol. Prog. Ser. **51:** 201–213.

———, H. P. GROSSART, H. PLOUG, AND B. SCHWEITZER. 2002. Microbial ecology of detrital aggregates in aquatic ecosystems. Aquat. Microb. Ecol. **28:** 175–211.

SMITH, D. C., G. F. STEWARD, R. A. LONG, AND F. AZAM. 1995. Bacterial mediation of carbon fluxes during a diatom bloom in a mesocosm. Deep-Sea Res. II, **42:** 75–97.

TORTELL, P. D., G. R. DITULLIO, D. M. SIGMANN, AND F. M. M. MOREL. 2002. CO_2 effects on taxonomic composition and nutrient utilization in an Equatorial Pacific phytoplankton assemblage. Mar. Ecol. Prog. Ser. **236:** 37–43.

WOLF-GLADROW, D., U. RIEBESELL, S. BURKHARDT, AND J. BIJMA. 1999. Direct effect of CO_2 concentration on growth and isotopic composition of marine plankton. Tellus **51B:** 461–476.

WOLFE, G. V., M. STEINKE, AND G. O. KIRST. 1997. Grazing-activated chemical defense in a unicellular marine alga. Nature **387:** 894–897.

ZAK, D. R., K. S. PREGITZER, P. S. CURTIS, AND W. E. HOLMES. 2000. Atmospheric CO_2 and the composition of soil microbial communities. Ecol. Appl. **10:** 47–59.

ZONDERVAN, I., B. ROST, AND U. RIEBESELL. 2002. Effect of CO_2 concentration on the PIC/POC ratio in the coccolithophore *Emiliania huxleyi* grown under light-limiting conditions and different day lengths. J. Exp. Mar. Biol. Ecol. **272:** 55–70.

Received: 19 April 2005
Accepted: 29 August 2005
Amended: 9 September 2005